

FFI RAPPORT

**MEASUREMENTS AND ANALYSIS OF
FLUCTUATIONS IN THE EARTH'S
MAGNETIC FIELD IN A COASTAL WATER
AREA - Originally presented at Marelec'97,
June 1997**

EIDEM Ellen Johanne

FFI/RAPPORT-2006/04011

**MEASUREMENTS AND ANALYSIS OF
FLUCTUATIONS IN THE EARTH'S MAGNETIC
FIELD IN A COASTAL WATER AREA - Originally
presented at Marelec'97, June 1997**

EIDEM Ellen Johanne

FFI/RAPPORT-2006/04011

FORSVARETS FORSKNINGSINSTITUTT
Norwegian Defence Research Establishment
P O Box 25, NO-2027 Kjeller, Norway

FORSVARETS FORSKNINGSINSTITUTT (FFI)
Norwegian Defence Research Establishment

UNCLASSIFIED

P O BOX 25
 NO-2027 KJELLER, NORWAY
REPORT DOCUMENTATION PAGE

SECURITY CLASSIFICATION OF THIS PAGE
 (when data entered)

1) PUBL/REPORT NUMBER FFI/RAPPORT-2006/04011	2) SECURITY CLASSIFICATION UNCLASSIFIED	3) NUMBER OF PAGES 20
1a) PROJECT REFERENCE FFI-IV/886/914	2a) DECLASSIFICATION/DOWNGRADING SCHEDULE -	
4) TITLE MEASUREMENTS AND ANALYSIS OF FLUCTUATIONS IN THE EARTH'S MAGNETIC FIELD IN A COASTAL WATER AREA - Originally presented at Marelec'97, June 1997		
5) NAMES OF AUTHOR(S) IN FULL (surname first) EIDEM Ellen Johanne		
6) DISTRIBUTION STATEMENT Approved for public release. Distribution unlimited. (Offentlig tilgjengelig)		
7) INDEXING TERMS IN ENGLISH:		
a) <u>Geomagnetic activity</u>		IN NORWEGIAN:
b) <u>Earth's magnetic field</u>		a) <u>Geomagnetisk aktivitet</u>
c) <u>Power spectral density</u>		b) <u>Jordmagnetfeltet</u>
d) <u>Noise reduction</u>		c) <u>Effektstetthetsspetrum</u>
e) _____		d) <u>Støyreduksjon</u>
		e) _____
THESAURUS REFERENCE:		
8) ABSTRACT Forsvarets forskningsinstitutt accomplished in September 1991 a pilot study investigating fluctuations in the earth's magnetic field in a coastal water area in Norway. The experimental data was collected during seven days using four bottom-mounted three-axial fluxgate magnetometers sampled at 2 Hz and the paper describes the experiment and some of the results found. The long-time series are analysed with respect to power spectral density, squared coherence and phase shifts/time delays. A subtraction filter is introduced to reduce the ambient noise. The results are compared with results from other, equivalent measurements of fluctuations in the geomagnetic field. This report was originally presented as a paper at the conference Marelec'97 in London, June 1997		
9) DATE 2006-12-28	AUTHORIZED BY This page only Elling Tveit	POSITION Director of Research

ISBN 978-82-464-1079-1

UNCLASSIFIED

SECURITY CLASSIFICATION OF THIS PAGE
 (when data entered)

CONTENTS

	Page
1 INTRODUCTION	7
2 EXPERIMENTAL	7
3 DIGITAL SIGNAL PROCESSING	8
4 RESULTS AND DISCUSSION	10
4.1 Time series	10
4.2 Power spectral densities (PSD)	10
4.3 Coherence	13
4.4 Phase shifts and time delays	15
4.5 Subtraction filtering	17
4.6 Herdla measuring range	18
4.7 Remarks regarding digital signal processing	19
5 CONCLUSIONS	20
References	20

MEASUREMENTS AND ANALYSIS OF FLUCTUATIONS IN THE EARTH'S MAGNETIC FIELD IN A COASTAL WATER AREA - Originally presented at Marelec'97, June 1997

1 INTRODUCTION

Magnetic detection of moving vessels can be improved by using a remote magnetometer if the spatial coherence of the ambient geomagnetic field is high. Simple differential techniques may reduce the geomagnetic field and enhance the magnetic signature of the vessel. In 1989 the SACLANT Undersea Research Centre set up an experiment off the west coast of Italy to investigate the spatial correlation of the earth's magnetic field (1). The results showed high coherence between the one sea-based magnetometer at 100 m depth and the two land-based magnetometers 600-625 m away.

Forsvarets forskningsinstitutt (FFI) accomplished as a pilot study a similar experiment in 1991 in a coastal water area in Norway. The paper describes the experiment and the data is analysed with respect to power spectral density, coherence and phase shifts. The results are compared with results from Italy and from other equivalent experiments. A subtraction filter is introduced to reduce the ambient field.

This report was originally presented as a paper at the conference Marelec'97 in London, June 1997. Only minor changes are done here.

2 EXPERIMENTAL

The experiment was set up in a sound South of the city of Bergen in Western Norway. The sound is 1200 m wide and oriented approximately north-south. There are islands on both sides of the sound, where the western islands make the border to the North Sea. The experimental data was collected during seven days in September 1991 using four gimballed, bottom-mounted three-axial fluxgate magnetometers of the type MUWS3 supplied by Dowty Magnetics, UK.

In the first of the two experimental phases, three sensors (M1, M2 and M3) were emplaced in the middle of the sound, separated at distances up to 310 m, see Figure 3.1, Table 3.1 and Table 3.2. The fourth sensor (LS) was located at the water's edge on a sub sea plateau 3 m below the sea level. Unfortunately, magnetic noise due to mechanical vibrations of the sensor was induced and impoverished the data.

In Phase II M1 remained emplaced in its original position. Station M4 was located 115 m south of M1, a land-based station (L) was located 5 m from the water's edge (1 m above sea level) and the last station was located 300 m from shore at station S.

In the paper the x-component (X) corresponds to magnetic North, the y-component (Y) to magnetic East and the z-component (Z) is positive downward. The declination of the magnetic field is approximately -6° in the area. Seven long-time series were recorded, of these three are analysed in the paper, see Table 3.3. Details of the experiment and data results from all the time series are reported in (2). However, the data processing in (2) differs from here.

3 DIGITAL SIGNAL PROCESSING

In order to study the fluctuations in the geomagnetic field, the disturbing influences from passing ships had to be removed from the time series. A "straight" line was interpolated between the manually detected start and end points of each ship influence.

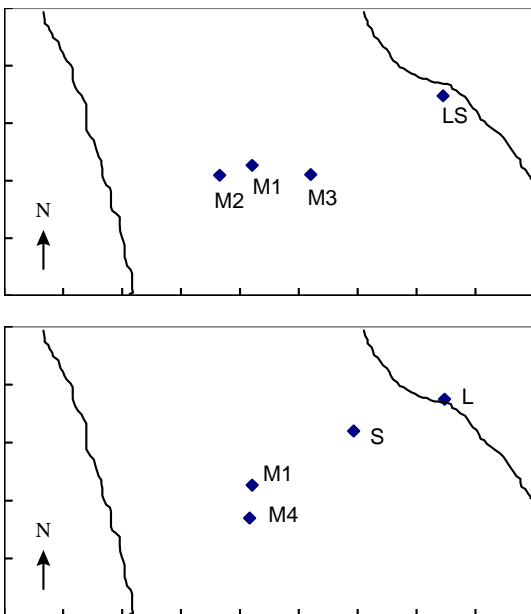


Figure 3.1 The magnetometer stations during Phase I (upper) and Phase II (lower). It is 200 m between the ticks.

M1-M2:	115 m	M1-M3:	200 m	M2-M3:	310 m
M1-LS:	690 m	M2-LS:	810 m	M3-LS:	525 m
M1-M4:	115 m	M1-L:	720 m	M1-S:	390 m
L-S:	330 m	M4-L:	780 m	M4-S:	465 m

Table 3.1 Horizontal distance between the stations.

Measurement Station					
M1	M2	M3	M4	LS	S
147 m	135 m	152 m	137 m	3 m	27 m

Table 3.2 Sensors depths during Phase I and Phase II (one station (L) was land-based in Phase II).

Phase	Time Series	Date Start	Time Start	Period (h)	Frequency (Hz)
I	C1	13/09/91	14:32	15	2
I	E1	15/09/91	15:27	15	2
II	H1	18/09/91	12:58	15	2

Table 3.3 Analysed time series (local times).

The signal processing was performed on a HP work station using IDL developed by Research, Inc. Systems. The one-sided power spectral density (PSD) was computed using 103 averages, Hanning window, 50% overlap and a batch length of $N=2048$ samples (resolution $\Delta f \sim 1$ mHz), according to (3)(4)

$$G_{xx}(f_k) = 2 \cdot \frac{1}{T} \cdot |X_T(f_k)|^2 \cdot Q^{-1}, \quad k \in \langle 0, \frac{N}{2} \rangle \quad (3.1)$$

$$X_T(f_k) = \Delta t \cdot \sum_{n=0}^{N-1} x(t_n) \cdot e^{-i2\pi nk/N} \quad (3.2)$$

where

$$Q = \frac{1}{N} \sum_{n=0}^{N-1} w^2(t_n) \quad (3.3)$$

$f_k = k\Delta f = k/T$ is the frequency, T is the length of the batch in seconds, $t_n = n\Delta t$ is the time, Δt is the sampling period, and $w(t)$ is the window function. The PSD is divided by the energy of the Hanning window $Q = 0.375$. The (squared) coherence, which varies between 0 and 1, gives a measure of how well two time series $x(t)$ and $y(t)$ are linearly related for each frequency. The coherence was computed using 209 averages, Hanning window, 50% overlap and a batch length of $N=1024$ samples ($\Delta f \sim 2$ mHz), according to

$$\gamma^2(f_k) = |G_{xy}(f_k)|^2 / (G_{xx}(f_k) \cdot G_{yy}(f_k)) \quad (3.4)$$

where

$$G_{xy}(f_k) = 2 \cdot \frac{1}{T} \cdot X_T(f_k) \cdot Y_T^*(f_k) \cdot Q^{-1} \quad (3.5)$$

represent the cross spectral density (CSD) of the time series. The phase of the CSD, $\Theta_{xy}(f_k)$, gives a measure of the phase shift between the two time series as a function of frequency. If the time series are linearly dependent, the phase is a linear function of the time delay τ between the series, as

$$\Theta_{xy}(f_k) = -2\pi\tau f_k \quad (3.6)$$

Hence, the slope of the phase gives the time delay. If the phase is positive, $x(t)$ lags $y(t)$, and visa versa.

4 RESULTS AND DISCUSSION

4.1 Time series

Figure 4.1 shows the three long-time series analysed in the paper, measured at station M1. The data is averaged over 15 s. The geomagnetic noise was high during the recording of C1, specially the last 8 h, with changes up to 120 nT within 20 min.

4.2 Power spectral densities (PSD)

1) *Analysis of the Mid-Sound Stations:* Table 4.1 gives the computed PSD of time series C1, E1 and H1 at three different frequencies. At 0.001 Hz the PSD is between 28-40 dB in the horizontal direction, and agrees with the results found in (1). The PSD of the z-component at 0.001 Hz is however much lower off the west coast of Italy, than in the Bergen area. The PSD found in (1) is ca. 18 dB, while the corresponding value in the FFI experiment is between 30-44 dB. The deviation agrees with the fact that the geomagnetic activity in the vertical direction is higher at northern latitudes than at mid-latitudes. The PSD decreases between 26-34 dB/decade in the interval 0.001-0.01 Hz, and 18-29 dB/decade in the interval 0.01-0.1 Hz, see Table 4.2. For frequencies above ~ 0.1 Hz, the sensor noise dominated the geomagnetic noise and the spectral levels are sensor- and axis-related.

The PSD of simultaneously measured x-components at the mid-sound stations are nearly equal. This is also the case for the y-components. However, the PSD of simultaneously measured z-components show station-dependent variations for frequencies above ~ 0.01 Hz, in such a way that station M1, which is not the deepest, has the lowest PSD of all the four mid-sound stations, see Figure 4.2.

The PSD of C1 is for all three mid-sound stations in Phase I much higher than the PSD of E1, showing that the geomagnetic activity was clearly higher during the recording of C1, see Figure 4.3.

2) *Land Station versus Sea Stations:* The PSD of the z-component is overall higher at the land station than at the mid-sound stations. In addition, during two of the three time series in Phase II (including H1), the PSD show that the land station was influenced by environmental noise, not observed at the mid-sound stations, see Figure 4.4.

Time series	Frequency					
	0.001 Hz		0.01 Hz		0.1 Hz	
	X,Y	Z	X,Y	Z	X,Y	Z
C1	40	43-44	12	9-11	-6	-8--20
E1	28	30-32	2	1--2	-20	-21
H1	31	32	4	-2	-19	-22

Table 4.1 The PSD (dB re $1nT^2/Hz$) at the mid-sound stations M1, M2 and M3 in Phase I, and M1 and M4 in Phase II (averaged over X and Y).

	Frequency Interval	
	0.001-0.01 Hz	0.01-0.1 Hz
X and Y	26-28	18-23
Z	31-34	18-20 (low geomagnetic activity) 19-29 (high geomagnetic activity)

Table 4.2 The decrease in PSD (dB/decade) with increasing frequency (at stations M1, M2, M3 and M4).

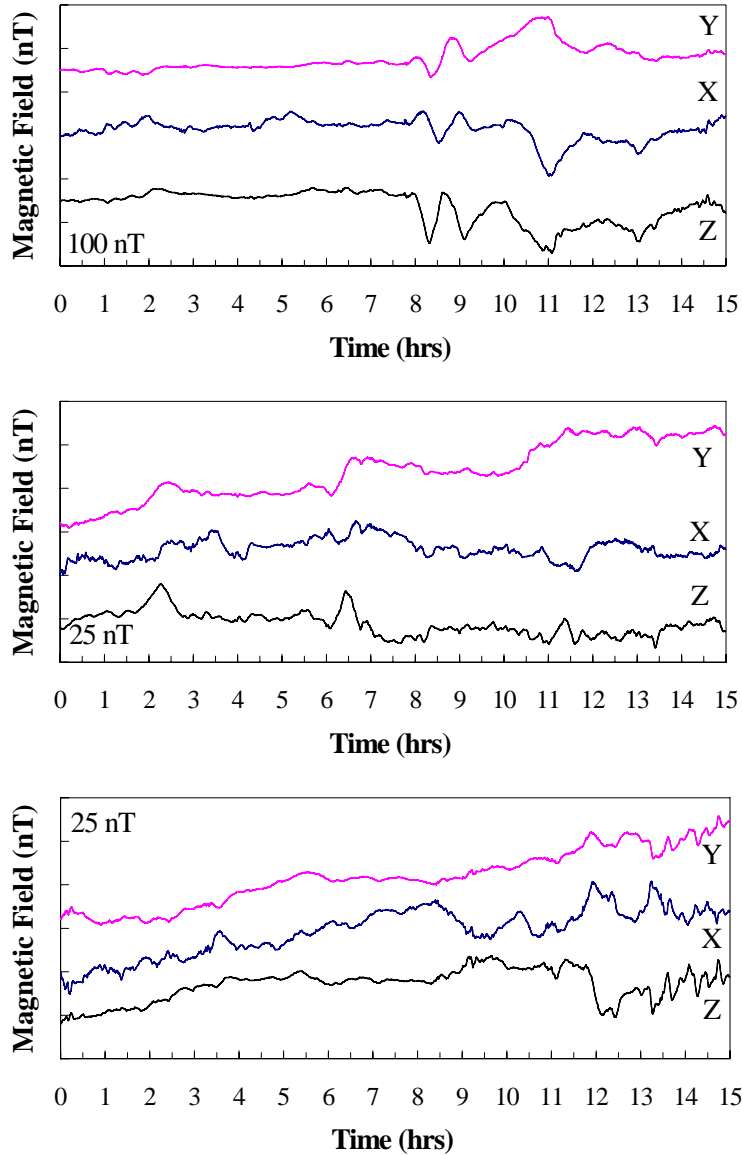


Figure 4.1 The time series C1 (upper), E1 (middle) and H1 (lower), measured at station M1. It is 100 nT/25 nT between the ticks.

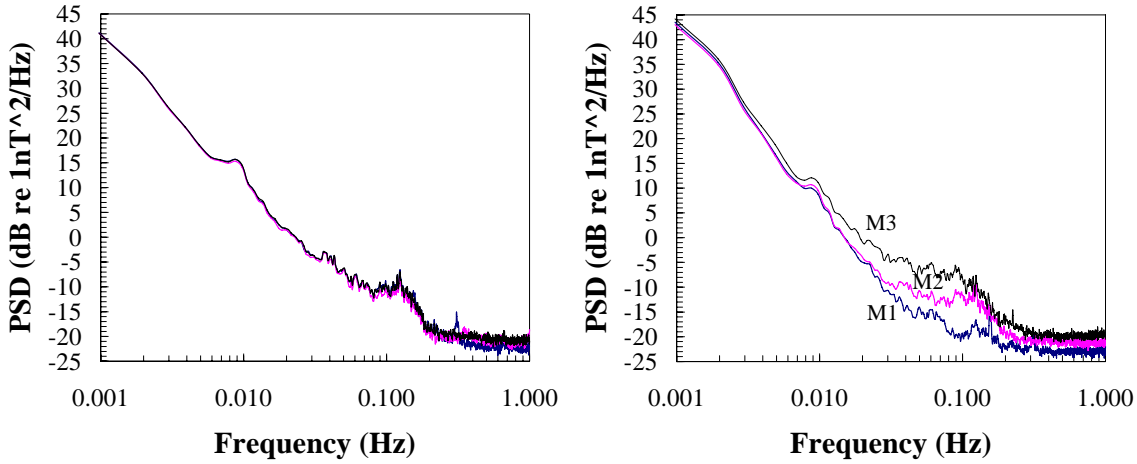


Figure 4.2 The PSD of the x - (left) and z - (right) components at stations M1, M2 and M3. Phase I, time series C1. The PSD of the x -components (and y -components) are nearly equal, while the PSD of the z -components deviate for frequencies above ~ 0.01 Hz.

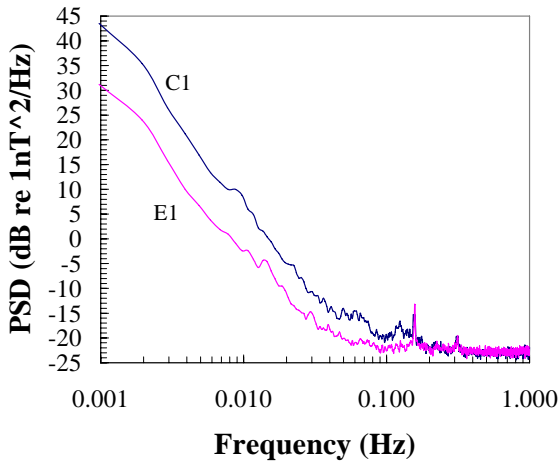


Figure 4.3 The PSD of the z -component at magnetometer station M1 during high (time series C1) and low (time series E1) geomagnetic activity. The data is averaged over 15 h.

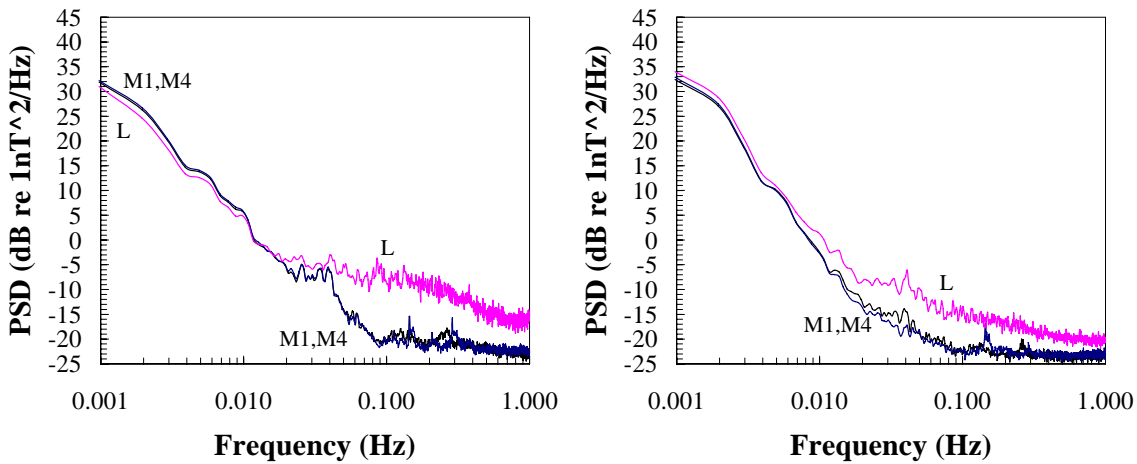


Figure 4.4 The PSD of the x - (left) and z - (right) components at stations M1, M4 and L. Phase II, time series H1.

4.3 Coherence

As in (1) the bandwidth that corresponds to the squared coherence above 0.5 is taken as a measure of coherence between two series, and the values are listed in Table 4.3. The squared coherence at 0.002 Hz is also tabulated.

1) *Analysis of the Mid-Sound Stations:* The x- and y-components are approximately equally coherent for mid-sound sensor pairs (as shown in Figure 4.5) and at 0.002 Hz the squared coherence is between 0.9-1.0. During high and low geomagnetic activity, the squared coherences are above 0.5 for frequencies up to 180 mHz and 50-65 mHz, respectively, see Figure 4.6. The z-component is in general less coherent than the horizontal components and during high geomagnetic activity the squared coherence is above 0.5 for frequencies up to only 30 mHz. The difference in coherence between the vertical and horizontal directions reduces with decreasing geomagnetic activity.

2) *Land station versus sea stations:* The spatial coherence for the sensor pair M1-L is lower than for the pair M1-M4, specially in the horizontal directions. The squared coherence of the y-component is above 0.5 for frequencies up to 65 mHz for the pair M1-M4, while the corresponding value for M1-L is only 10 mHz, see Figure 4.7. And at 0.002 Hz the squared coherence is only 0.8 for M1-L. This indicates it would be better to use a nearby sea sensor as reference than a remote land sensor, in order to enhance magnetic ship influences. The disadvantage is that both the sea sensors may observe the ship influences.

Off the west coast of Italy (1), the squared coherence of the z-component for the land-sea pair (separated 625 m) was found to be better than in the FFI experiment: above 0.5 for frequencies up to 40 mHz (averaged over 18 h) - even if the geomagnetic noise in the vertical direction is much lower than in the Bergen area.

Series: C1	Component		
Sensor pair	X	Y	Z
M1-M2	1.0 [175]	1.0 [180]	1.0 [30]
M1-M3	1.0 [175]	1.0 [180]	1.0 [30]
M2-M3	1.0 [175]	1.0 [180]	0.95 [20]
Series: E1	Component		
Sensor pair	X	Y	Z
M1-M2	1.0 [50]	0.9 [50]	1.0 [25]
M1-M3	1.0 [50]	0.9 [50]	0.95 [20]
M2-M3	1.0 [50]	1.0 [50]	0.95 [20]
Series: H1	Component		
Sensor pair	X	Y	Z
M1-M4	1.0 [55]	1.0 [65]	1.0 [20]
M1-L	0.9 [15]	0.8 [10]	0.95 [15]

Table 4.3 The squared coherence at frequency 0.002 Hz and the bandwidth where the squared coherence is above 0.5 (mHz) in brackets.

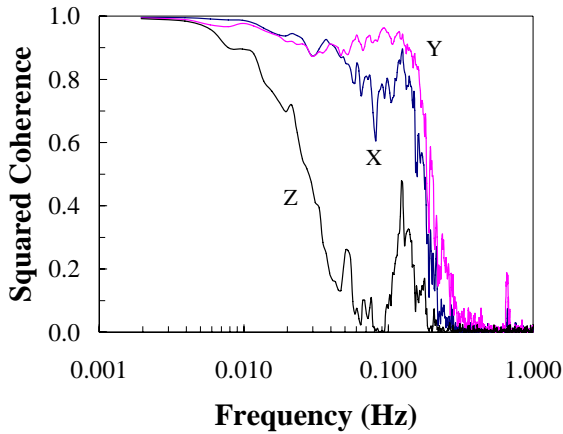


Figure 4.5 The squared coherence of the x-, y- and z-components for the sensor pair M1-M2. Time series C1, Phase I. The spatial coherence is lower in the z-component, then in the x- and y-components at the mid-sound stations.

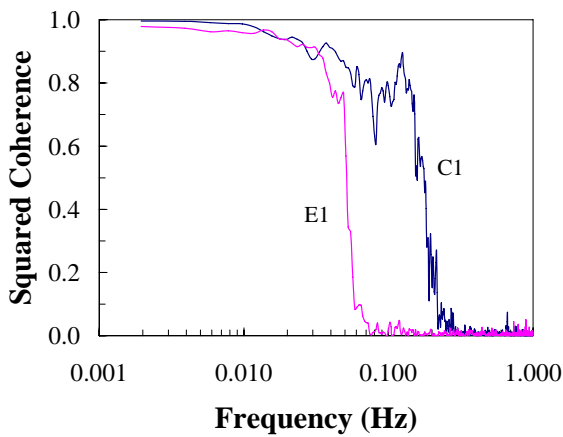


Figure 4.6 The squared coherence of the x-component for the sensor pair M1-M2 during high (time series C1) and low geomagnetic activity (time series E1). In the vertical direction, the coherence is much less influenced by the amount of geomagnetic activity.

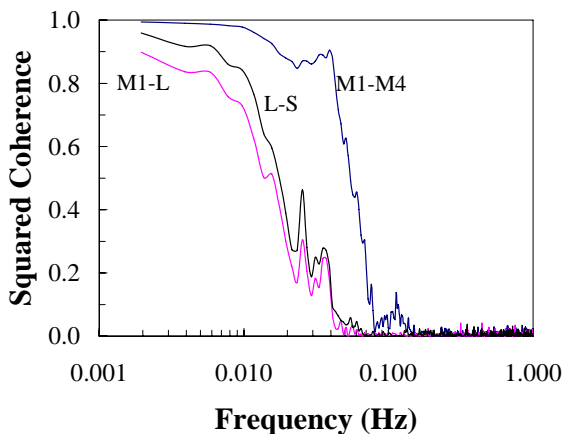


Figure 4.7 The squared coherence of the x-components for the sensor pairs M1-M4, M1-L and L-S. Time series H1. The spatial coherence is higher for the sea-sea pair than for the sea-land pairs.

4.4 Phase shifts and time delays

The phase of the CSD in the x-component is approximately zero for all the sensor pairs, indicating no time delays in this direction. In the y-component phase shifts are present between the mid-sound stations and the land station, see Figure 4.8. Assuming a linear relationship between the time series for frequencies below 0.01 Hz, the time delay for M1-L is estimated to be up to 50-60 s (distance 720 m) in the y-component, as illustrated in Figure 4.9. In the z-component phase shifts are present among the mid-sound stations - and between the land station and the mid-sound stations, see Figure 4.10. The time delay in the z-component for M2-M3 (310 m apart) is estimated to be up to 20-25 s, the western sensor lagging the eastern. Extracts of time series C1 and H1, showing time delays, are presented in Figure 4.11 and Figure 4.12.

A later experiment with eight fibre-optic magnetometers in the same sound has confirmed the presence of the time delays (and the deviations in PSD between mid-sound stations in the z-component) (5).

Efforts have therefore been invested to see if the time delays are dependent on local time or on the tidal current (which is north-going on rising sea and south going on falling sea), but no correlation has been found.

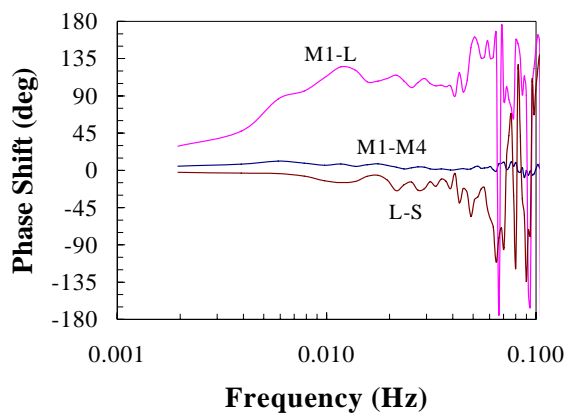


Figure 4.8 The phase of the cross spectral density of the y-component for different sensor pairs. Time series H1. The sea-land pair M1-L was 720 m apart, while the sea-sea pair M1-M4 was 115 m apart.

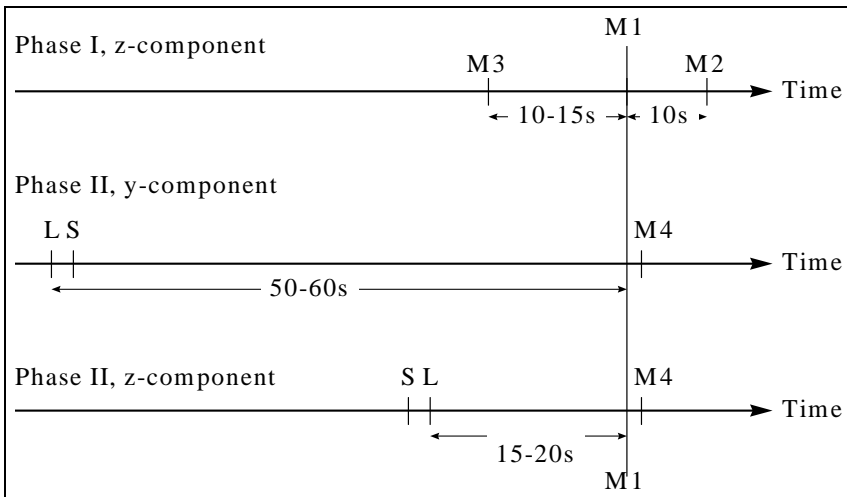


Figure 4.9 Estimated time delays between the magnetometer stations. The delays are estimated from the slope of the phase of the cross spectral densities (frequency interval 0.002-0.01 Hz). Time series C1, E1 and H1. In Phase II, station M1 lagged the land station L 720 m north-east of M1 by 50-60 s in the y-component.

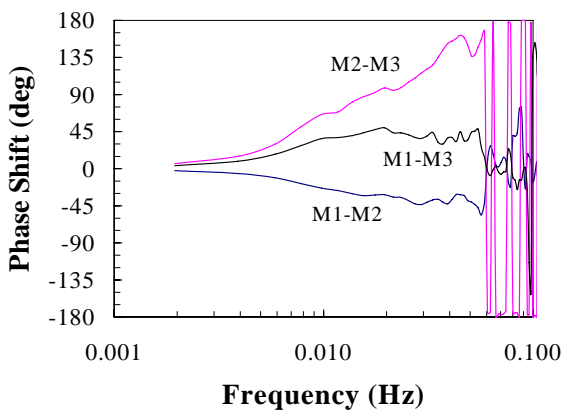


Figure 4.10 The phase of the cross spectral density of the z-component for different sensor pairs. Time series C1. The sensors were up to 310 m apart.

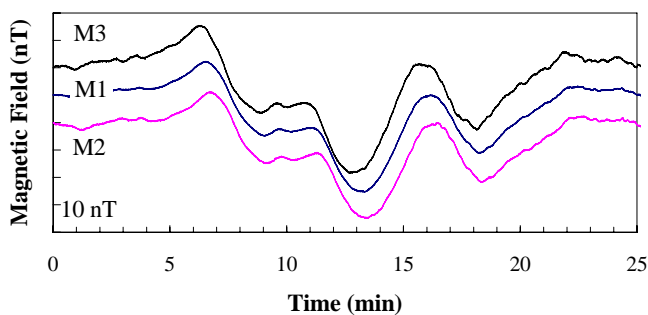


Figure 4.11 Extract of time series C1 showing that station M3 (east) measured magnetic fluctuations in the z-component earlier than station M1 and M2 (west). Time series C1.

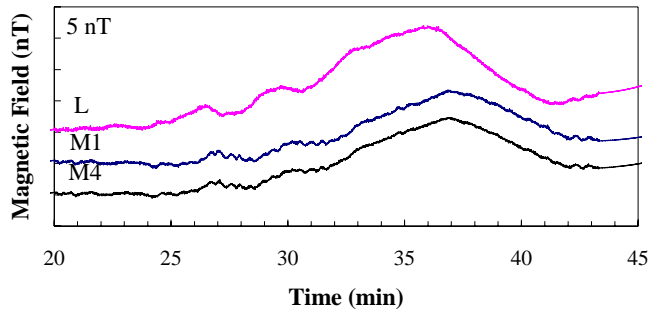


Figure 4.12 Extract of time series H1 showing that station L measured magnetic fluctuations in the y-component earlier than station M1 and M4 (720-780 m south-west of L).

4.5 Subtraction filtering

When the coherence between two stations is high, then the geomagnetic noise may be removed by subtraction filtering. The use of a subtraction filter at station M1 (reference station M2), reduces the PSD with 14-24 dB at 0.001 Hz, see Figure 4.13 and Table 4.4.

At the lower frequencies, the filter is more effective in the horizontal directions than in the z-direction. The benefit of using a subtraction filter decreases with increasing frequency. In fact, at higher frequencies the filter may function in opposite of its intention, due to uncorrelated sensor noise.

If the land station L is used as reference, the benefit of using the subtraction filter is much lower or negative, even in the x-component where the phase shifts are negligible, see Figure 4.14. Hence, the analysis indicates it is much better to use M4 than L as a reference for station M1, in order to reduce the ambient geomagnetic field and enhance magnetic ship signatures at station M1.

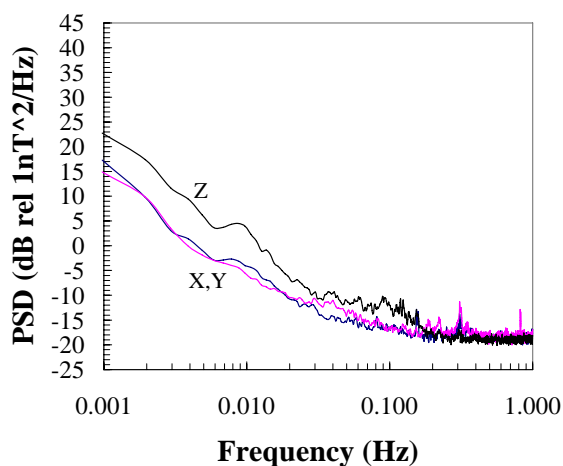


Figure 4.13 The PSD of the x-, y- and z-component at station M1 after subtraction filtering (reference station M2). Time series C1.

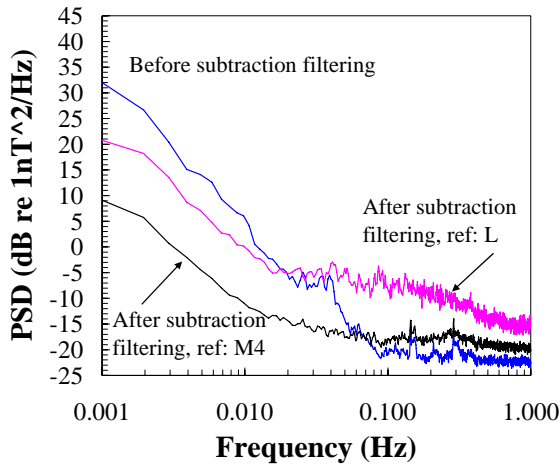


Figure 4.14 The PSD of the x -component at station M1 before and after subtraction filtering (reference stations M4 and L). Time series H1.

TS	Ref.	Frequency					
		0.001 Hz		0.01 Hz		0.1 Hz	
		X,Y	Z	X,Y	Z	X,Y	Z
C1	M2	24	20	17	4	11	-7
E1	M2	16	14	12	4	-3	-4
H1	M4	21	21	15	6	-1	-3
H1	L	X:11 Y:3	13	X:6 Y:-3	0	X:-11 Y:-11	-8

Table 4.4 The decrease in PSD due to subtraction filtering (dB re $1nT^2/Hz$) of the X-, Y- and z-components at station M1 using reference stations M2, M4 and L (averaged over x and y).

4.6 Herdla measuring range

After the pilot study was ended, the MUWS3 sensors were moved to a sound North of the city of Bergen in Western Norway. Analysing time series from this range, no phase shifts are found between the four sea-based stations separated at distances up to 315 m in none of the directions!

The time series recorded 20.-21. January 1994 (starting time 15:19) is shown in Figure 4.15. Sensor S3 was located at depth 91 m, while S4 was located 210 m north-west, at depth 84 m. The geomagnetic activity was not high, nor low during this recording, according to the PSD given in Table 4.4. Using a subtraction filter, the PSD reduces with 29-34 dB at 0.001 Hz, see Table 4.5. This is much better than in the FFI experiment from 1991, where the reduction was 14-24 dB. Further, as shown in Figure 4.16, the phase of the CSD is approximately zero for frequencies up to 0.4 Hz in all three directions, indicating no time delays between the two sea-based stations S3 and S4 210 m apart.

	Frequency					
	0.001 Hz		0.01 Hz		0.1 Hz	
	X,Y	Z	X,Y	Z	X,Y	Z
Before	34	41	7	10	-17	-14
After	5	7	-7	-6	-15	-12

Table 4.5 The PSD ($\text{dB re } 1\text{nT}^2/\text{Hz}$) at the sea station S3 before and after subtraction filtering (ref: s4), Time series j94, Herdla (averaged over X and Y).

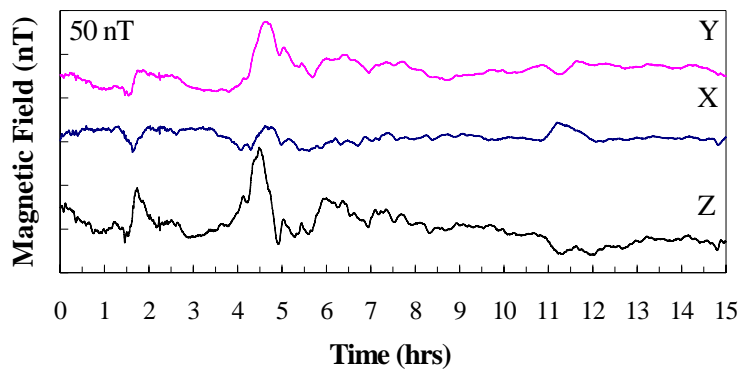


Figure 4.15 Time series J94 measured at Herdla range (station S3). Starting time 20. January 1994, 15:19 local time. The data is averaged over 15 s. The ticks are 50 nT apart.

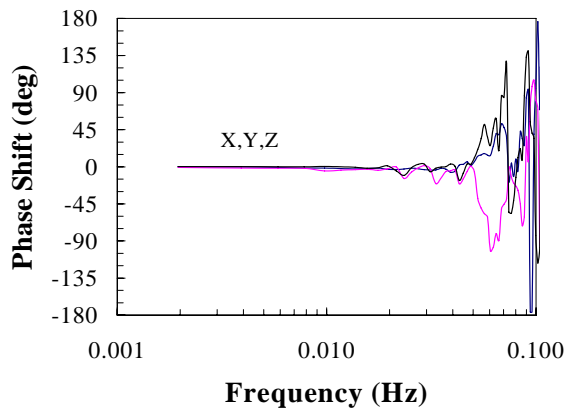


Figure 4.16 The phase of the cross spectral density of the x-, y- and z-component for the sensor pair S3-S4 at Herdla range North of the city of Bergen. Time series J94.

4.7 Remarks regarding digital signal processing

One disadvantage when analysing the data with respect to fluctuations in the earth's magnetic field, is the many influences from passing vessels, which amount to 10-15 % of the time. The interpolation of "straight" lines replacing the disturbing ship influences introduces unknown effects on the data set. Even so, this was thought to be better than to only study short cuts with no ship influences or to fit together the no-ship-influence-periods, giving jumps in the data set.

The choice of using Hanning window in the FFT's is made in order to have the possibility to compare the data with results reported in (1). It is seen that other window functions could modify the spectral densities etc.

5 CONCLUSIONS

Regarding the mid-sound stations, the power spectral density (PSD) at frequency 0.001 Hz is between 28-44 dB, dependent on the direction of the field (horizontal/vertical) and on the amount of geomagnetic noise. The decrease in PSD is between 26-34 dB/decade in the interval 0.001-0.01 Hz, and between 18-29 dB/decade in the interval 0.01-0.1 Hz. The PSD of the z-components show station-dependent variations for frequencies above ~0.01 Hz. The PSD of the z-component is overall higher at the land station than at the mid-sound stations.

The PSD of simultaneously measured x- or y-components at the mid-sound stations are nearly equal. The x- and y-components are approximately equally coherent for the mid-sound sensor pairs, with a squared coherence above 0.5 for frequencies up to 180 mHz during high geomagnetic activity. The z-component is less coherent than the horizontal components and the squared coherence is above 0.5 for frequencies up to only 30 mHz, at best. The coherence for the land-sea pairs are in general bad, indicating it is better using a nearby sea station as reference than a remote land station, in order to reduce the ambient geomagnetic field and enhance magnetic ship influences. No time delays are present in the x-component. In the y-component time delays up to 50-60 s is estimated for the pair M1-L, in the frequency interval 0.002-0.01 Hz. In the z-component time delays are estimated for the sea-sea pairs, indicating the western sensor lagging the eastern with up to 20-25 s (distance 310 m).

The use of a subtraction filter at station M1 (reference station M2 or M4, both 115 m apart), reduces the PSD with 14-24 dB at frequency 0.001 Hz, but much lesser if L is the reference station. The time delays are confirmed in a later experiment at the same range. The delays are not observed between sea-based stations at another range in the same coastal water area.

References

- (1) J.P. Hermand, "The Formiche '89 experiment: Spatial and Temporal Variability of Magnetic Ambient Noise". Italy: SACLANTCEN REPORT SR-176, March 1991.
- (2) Eidem, Ellen Johanne and Zimmer, Even (1992): The Earth's Magnetic Field in a Coastal Water Area: Measurements and Analysis, FFI/NOTAT-92/2020
- (3) S. Kay and S. Marple, "Spectrum Analysis - A Modern Perspective", *Proceedings of the IEEE*, vol. 69, no. 11, November 1981, pp 1380-1419.
- (4) T.S. Durrani and J.M. Nightingale, "Data windows for digital spectral analysis", *Proceedings of the IEE*, vol. 119, no. 3, March 1972, pp 343-352.
- (5) F. Bucholtz et al, "Multichannel Fiber-Optic Magnetometer System for Undersea Measurements", *Journal of Lightwave Technology*, vol. 13, no. 7, July 1995, pp. 1385-1395.